JACS
JOURNAL OF THE AMERICAN CHEMICAL SOCIETY
Article
pubs.acs.org/JACS
Terms of Use

Modulated Protonation of Side Chain Aminoethylene Repeats in N-Substituted Polyaspartamides Promotes mRNA Transfection

Hirokuni Uchida,[†] Keiji Itaka,[†] Takahiro Nomoto,[‡] Takehiko Ishii,[‡] Tomoya Suma,[∥] Masaru Ikegami,[†] Kanjiro Miyata,[†] Makoto Oba,[⊥] Nobuhiro Nishiyama,[#] and Kazunori Kataoka*[,†,‡,§]

[†]Center for Disease Biology and Integrative Medicine, Graduate School of Medicine, [‡]Department of Bioengineering, Graduate School of Engineering, and [§]Department of Materials Engineering, Graduate School of Engineering, The University of Tokyo, 7-3-1 Hongo, Bunkyo, Tokyo 113-8656, Japan

[∥]Department of Chemical and Biomolecular Engineering, The University of Melbourne, Victoria 3010, Australia

[⊥]Graduate School of Biomedical Sciences, Nagasaki University, 1-14 Bunkyo-machi, Nagasaki 852-8521, Japan

[#]Polymer Chemistry Division, Chemical Resources Laboratory, Tokyo Institute of Technology, R1-11, 4529 Nagatsuta, Midori-ku, Yokohama 226-8503, Japan

S *Supporting Information*

ABSTRACT: Fine-tuning of chemical structures of polycation-based carriers (polyplexes) is an attractive strategy for safe and efficient mRNA transfaction. Here, mRNA polyplexes comprising N-substituted polyaspartamides with varied numbers of side chain aminoethylene repeats were constructed, and their transfection ability against human hepatoma cells was examined. Transfection efficacy clearly correlated with the number of aminoethylene repeats: polyplexes with odd number repeats (PA-Os) produced sustained increases in mRNA expression compared with those with even number repeats (PA-Es). This predominant efficacy of PA-Os over PA-Es was contradictory to our previous findings for pDNA polyplexes prepared from the same N-substituted polyaspartamides, that is, PA-Es revealed superior transfection efficacy of pDNA than PA-Os. Intracellular FRET analysis using flow cytometry and polyplex tracking under confocal laser scanning microscopy revealed that overall transfection efficacy was determined through the balance between endosomal escaping capability and stability of translocated mRNA in cytoplasm. PA-Es efficiently transported mRNA into the cytoplasm. However, their poor cytoplasmic stability led to facile degradation of mRNA, resulting in a less durable pattern of transfection. Alternatively, PA-Os with limited capability of endosomal escape eventually protect mRNA in the cytoplasm to induce sustainable mRNA expression. Higher cytoplasmic stability of pDNA compared to mRNA may shift the limiting step in transfection from cytoplasmic stability to endosomal escape capacity, thereby giving an opposite odd−even effect in transfection efficacy. Endosomal escaping capability and nuclease stability of polyplexes are correlated with the modulated protonation behavior in aminoethylene repeats responding to pH, appealing the substantial importance of chemistry to design polycation structures for promoted mRNA transfection.

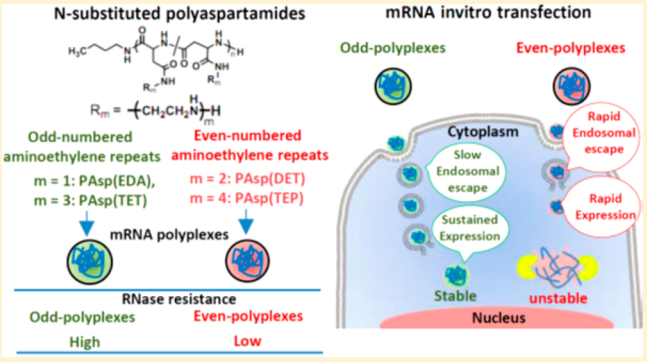

INTRODUCTION

Messenger RNA (mRNA) has attracted attention as a novel nucleic acid medicine for gene regulation therapy.[1,2] However, wide application has been limited because of the extremely labile nature of mRNA under physiological conditions, which hamper efficient and sustained delivery of mRNA. Polycations have been extensively studied for the delivery of nucleic acids because of their electrostatic interactions with nucleic acids, allowing the complex formation, which were termed "polyplex".[3−6] Polyplex systems can enhance cellular uptake and protect nucleic acids from nuclease digestion. Therefore, this system is considered to have high feasibility for effective delivery of mRNA, although few studies have focused on the chemical design of polycations customized for mRNA delivery.

Fine-tuning of chemical structures of polycations could dramatically improve the capability of polyplexes to overcome several barriers for successful polyplex transfection.[7−11] One of the critical barriers of polyplex transfection is inefficient translocation from endosomes into cytoplasm.[12] In our previous study directing to develop plasmid DNA (pDNA)-loaded polyplexes, the systematically varied number of aminoethylene repeats in the side chain on N-substituteted polyaspartamides revealed a marked impact on transfection efficiency of pDNA polyplexes. The polycations with an even number of aminoethylene repeats gave rise to polyplexes with

Received: June 20, 2014
Published: August 18, 2014

   dx.doi.org/10.1021/ja506194z | J. Am. Chem. Soc. 2014, 136, 12396−12405

substantially higher transfection efficacy than those with an odd number of repeats.[9] This odd−even effect correlated with endosomal escape of polyplexes, which was greater for polyplexes with an even number of aminoethylene repeats. These observations can be ascribed to its potential to undergo an abrupt increase in the protonation degree of the side chain aminoethylene repeats in response to a decrease in the pH from physiological condition (∼7.4) to acidic condition (∼5.5), which corresponds to endosomal compartment.

This odd−even effect of N-substituted polyaspartamides was expected to remain intact during application for delivery of mRNA. Unprecedentedly, mRNA polyplexes with an odd number of aminoethylene repeats revealed much more durable and higher transfection efficacy than those with an even number of repeats. These unique findings are apparently contradictory to pDNA results, motivating us to carry out the present study to clarify the key structural parameters that determine the transfection efficacy of mRNA polyplexes formed using these polycations. The present data demonstrate the importance of fine-tuning in chemistry to regulate each key step that is involved in mRNA transfection toward the maximized efficacy.

EXPERIMENTAL SECTION

Materials. β-Benzyl-L-aspartate *N*-carboxyanhydride (BLA-NCA) was purchased from Chuo Kasei Co. Ltd. (Osaka, Japan). *N*-Methyl-2-pyrrolidone (NMP) was purchased from Nakalai Tesque Inc. (Kyoto, Japan). *N*,*N*-Dimethylformamide (DMF), dichloromethane (CH_2Cl_2), *n*-butylamine, ethylenediamine (EDA), diethylenetriamine (DET), triethylenetetramine (TET), tetraethylenepentamine (TEP), tris-(hydroxymethyl)aminomethane (Tris), 2-[4-(2-hydroxyethyl)-1-piperazinyl]ethanesulfonic acid (HEPES), and 2-morpholinoethanesulfonic acid monohydrate (MES) were purchased from Wako Pure Chemical Industries, Ltd. (Osaka, Japan). NMP, DMF, CH_2Cl_2, EDA, DET, TET, and TEP were used after conventional distillation. Dulbecco's modified Eagle's medium (DMEM) was purchased from Sigma-Aldrich Co. (St. Louis, MO). A plasmid DNA (pDNA) encoding Gaussia luciferase (GLuc) was purchased from New England BioLabs (Ipswich, CA). NucleoBond Xtra Maxi Plus for purification of competent DH5α *Escherichia coli* was purchased from Clontech Laboratories, Inc. (Mountain View, CA). Label IT Cy3 Labeling Kit and Label IT Cy5 Labeling Kit were purchased from Mirus Bio Corporation (Madison, WI). The transfection reagent ExGen 500 (linear polyethylenimine) was purchased from Fermentas LLC (Harrington Court, Canada). 96-Well and 12-well culture plates were purchased from Becton Dickinson Labware (Franklin Lakes, NJ). Human hepatoma cells (Huh-7) and fibroblast-like cell line (NIH3T3) were obtained from RIKEN Bioresource Center (Tsukuba, Japan). Fetal bovine serum (FBS) was purchased from MP Biomedicals, Inc. (Illkirch, France). Renilla Luciferase Assay System Kits were purchased from Promega Co. (Madison, WI). Cell Counting Kit-8 was purchased from Dojindo Laboratories (Kumamoto, Japan). CellLight Lysosomes-GFP and BacMam 2.0 were purchased from Molecular Probes (Eugene, OR).

Synthesis of Poly(β-benzyl-L-aspartate) (PBLA). PBLA was synthesized as previously reported.[8−10] In brief, BLA-NCA (1.2 g, 5 mmol) was dissolved in DMF (2 mL) and diluted with CH_2Cl_2 (20 mL), and *n*-butylamine diluted with CH_2Cl_2 (0.045 mL, 0.045 mmol) was added to initiate ring opening polymerization of NCA. The reaction solution was stirred for 2 days at 35 °C. All procedures were performed under an atmosphere of dry argon. PBLA was precipitated in an excess of *n*-hexane/AcOEt (6:4) and was filtered and dried in vacuo. The polydispersity (M_w/M_n) of PBLA was determined to be 1.06 using a gel permeation chromatography (GPC) system (HLC-8220, TOSOH Co., Tokyo, Japan) equipped with TSKgel columns (SuperAW4000 and SuperAW3000 × 2, TOSOH Co., Tokyo, Japan) and an internal refractive index (RI) detector at 40 °C. NMP containing 50 mM lithium bromide was used as eluent. PEG standards were used for the calibration (data not shown). The ^{1}H nuclear magnetic resonance (NMR) spectrum of PBLA in d_6-DMSO at 80 °C was recorded on a JEOL EX300 spectrometer (JEOL, Tokyo, Japan), and the degree of polymerization was confirmed to be 102 from the peak intensity ratio of methyl protons of the *n*-butyl terminus ($CH_3CH_2CH_2CH_2-$, δ = 0.9 ppm) to aromatic protons of benzyl esters ($C_6H_5CH_2-$, δ = 7.3 ppm; data not shown).

Synthesis of Poly[*N*-(2-aminoethyl)aspartamide] (PAsp(EDA)), Poly{*N*-[*N*′-(2-aminoethyl)-2-aminoethyl]aspartamide} (PAsp(DET)), Poly(*N*-{*N*′-[*N*″-(2-aminoethyl)-2-aminoethyl]-2-aminoethyl}aspartamide) (PAsp(TET)), and Poly[*N*-(*N*′-{*N*″-[*N*‴-(2-aminoethyl)-2-aminoethyl]-2-aminoethyl}-2-aminoethyl)aspartamide] (PAsp(TEP)). N-Substituted polyaspartamides were prepared by aminolysis of PBLA. Lyophilized PBLA (200 mg) was dissolved in NMP (2 mL) and cooled to 0 °C. In another reaction tube, EDA, DET, TET, or TEP (5 mL, 50-fold molar excess over benzyl ester units) was diluted 2-fold with NMP and cooled to 0 °C. The PBLA solution was then added dropwise, and after 1 h reaction 1 N aqueous HCl was added dropwise (5 mL, equimolar concentration to the added amino groups) at <10 °C. Mixtures were then dialyzed (MWCO: 6−8000) at 4 °C against a 0.01 N HCl aqueous solution for 1 day and then against deionized water for an additional day. The final solution was lyophilized to obtain PAsp(EDA), PAsp(DET), PAsp(TET), or PAsp(TEP). In each reaction, quantitative conversion of benzyl ester groups to $-CO-(NHCH_2CH_2)_{1-4}-NH_2$ groups was confirmed using ^{1}H NMR with a polymer concentration of 10 mg/mL D_2O, at 70 °C.

Preparation of mRNA. To perform in vitro transcription (IVT) of GLuc, a protein-expressing fragment of GLuc was cloned into a pSP73 vector (Promega) to give expression under a T7 promoter and then linearized with Nde I for use as an IVT template. IVT was performed using the mMESSAGE mMACHINE T7 Ultra Kit (Ambion, Invitrogen, Carlsbad, CA) according to the manufacturer's protocol. Transcribed mRNA was purified using the RNeasy Mini Preparation Kit (Qiagen, Hilden, Germany), and mRNA concentrations were determined using a spectrophotometer at 260 nm.

Preparation of Polyplexes Containing mRNA. The polycations PAsp(EDA), PAsp(DET), PAsp(TET), or PAsp(TEP) and mRNA were dissolved separately in 10 mM HEPES buffer. The concentration of nucleic acid was set at 50 μg/mL, and that of polycation was adjusted at the residual molar ratio of the polycation amino groups to mRNA phosphate groups (N/P) = 10. Solutions of polycation and mRNA were mixed at a ratio of 1:2 to obtain polyplex solutions with a final mRNA concentration of 33.3 μg/mL. ExGen 500/mRNA polyplex solution was prepared according to the manufacturer's protocol. Size and ζ-potential measurements of mRNA polyplexes were carried out using Zetasizer nanoseries (Malvern Instruments Ltd., Worcestershire, U.K.). For measuring polyplex size, a small glass cuvette (ZEN2112, Malvern Instruments Ltd.) was used. The obtained data were analyzed by using a cumulant method, and the hydrodynamic diameter of the polyplex was calculated with the Stokes−Einstein equation. For ζ-potential measurement, a folded capillary cell (DTS 1060, Malvern Instruments Ltd.) was used. The ζ-potential was calculated from the obtained electrophoretic mobility by applying the Smoluchowski equation.

Transfection of mRNA Polyplexes toward Huh-7 Cells. Huh-7 cells were cultured in DMEM containing 10% FBS at 37 °C in a humidified atmosphere containing 5% CO_2. For transfection, the cells were seeded onto 96-well culture plates (2500 cells/well) and were incubated overnight in DMEM containing 10% FBS (100 μL). Prior to transfection, the medium was replaced with an equal volume of fresh medium. Polyplex solutions containing mRNA were then added to each well (250 ng of mRNA/well). GLuc expression was evaluated according to photoluminescence intensity using the Renilla Luciferase Assay System and a Luminometer Glomax 96 (Promega Co.) from 3 to 72 h after transfection (n = 4). Cytotoxicity was assessed using a Cell Counting Kit-8 according to the manufacturer's protocol. Data are presented relative (%) to values from nontransfected control cells (n = 4).

dx.doi.org/10.1021/ja506194z | J. Am. Chem. Soc. 2014, 136, 12396−12405

Scheme 1. Preparation of N-Substituted Polyaspartamides

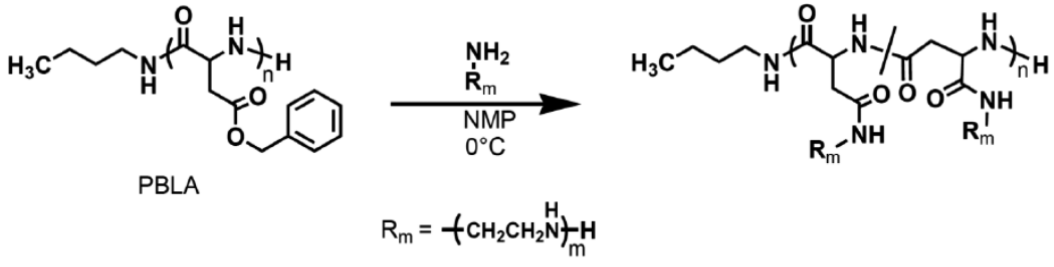

Confocal Laser Scanning Microscope (CLSM) Imaging of Polyplex Localization Inside Cells. The Label IT Cy3 Labeling Kit was used to label mRNA with Cy3 according to the manufacturer's protocol. Huh-7 cells (50 000 cells/dish) were seeded on 35 mm glass-based dishes (Iwaki, Tokyo, Japan) and were incubated overnight in 1 mL of DMEM containing 10% FBS. The medium was replaced with 1 mL of fresh medium, and 90 μL of polyplex solution containing 3 μg of Cy3-labeled mRNA (N/P = 10) was added. At 12, 24, and 48 h after transfection, the intracellular distribution of Cy3-labeled mRNA was observed using CLSM with costaining of acidic late endosomes and lysosomes using LysoTracker Green (Molecular Probes, Eugene, OR) and cell nuclei using Hoechst 33342 (Dojindo Laboratories, Kumamoto, Japan). CLSM imaging was performed using a LSM 510 instrument (Carl Zeiss, Oberlochen, Germany) with a 63× objective (C-Apochromat, Carl Zeiss, Germany) at excitation wavelengths of 488 nm for LysoTracker Green, 543 nm for Cy3, and 710 nm (MaiTai laser for 2-photon imaging) for Hoechst 33342.

Colocalization ratios of Cy3-labeled mRNA with late endosomes and lysosomes were calculated as follows:

$$\text{colocalization ratio} = \text{Cy3 pixels}_{\text{colocalization}}/\text{Cy3 pixels}_{\text{total}}$$

where Cy3 $\text{pixels}_{\text{colocalization}}$ represents the number of Cy3 pixels overlapping with LysoTracker Green, and Cy3 $\text{pixels}_{\text{total}}$ represents the total number of Cy3-positive pixels in the cell. For each condition, colocalization ratios were calculated from 10 individual cells, and the data are presented as mean ± standard error of the mean.

Hemolysis Assay. Murine erythrocytes were collected in heparin solution (10 000 units/mL) and were centrifuged at 600*g* for 5 min. The pellet was washed several times with PBS by centrifugation at 600*g* for 10 min, and finally resuspended in 1 mL of 20 mM HEPES (pH 7.4), 20 mM MES (pH 5.5), or 20 mM MES (pH 5.0) buffers containing 130 mM NaCl. PAsp(EDA), PAsp(DET), PAsp(TET), PAsp(TEP), and ExGen 500 polymer solutions were added to erythrocyte solutions at a residual amino group concentration of 5 mM, and were incubated in a shaking container at 37 °C for 30 min. After centrifugation (600*g* for 5 min), liberated hemoglobin levels were determined using colorimetric analyses of supernatants at 575 nm with a NanoDrop instrument (ND-1000 spectrophotometer, NanoDrop Technologies Inc., Wilmington, DE). To determine values for 100% hemolysis, erythrocyte solutions were lysed with 0.2 wt % Tween20. Data are presented as mean ± standard error of the mean from four samples.

Flow Cytometry Analysis to Measure Fluorescence Resonance Energy Transfer (FRET) in Cy3/Cy5-Labeled mRNA. Label IT Cy3 Labeling Kit and Label IT Cy5 Labeling Kit were used to simultaneously label mRNA with Cy3 and Cy5 with slight modification to the manufacturer's protocol. Huh-7 cells (40 000 cells/well) were seeded on 12-well culture plates and incubated for 24 h in DMEM containing 10% FBS (1 mL). Medium was replaced with an equal volume of fresh medium and 60 μL of polyplex solution containing 2 μg of Cy3/Cy5 double-labeled mRNA (N/P = 10) was added. After 8, 24, and 48 h incubation, the cells were washed twice with cold PBS and collected as suspension by trypsinization. The collected cells were centrifuged at 100*g* for 2 min and resuspended in PBS. The cells were sieved with a cell strainer prior to flow cytometry analysis. Fluorescence intensity of the cells was monitored and evaluated with a BD LSR II instrument (BD Biosciences, Franklin Lakes, NJ) equipped with FACSDiva software (BD Biosciences) using a 488 laser for excitation and a 660/20 nm filter. Data are presented as the mean ± standard error of the mean from three samples.

CLSM Imaging Analyses to Measure Fluorescence Resonance Energy Transfer (FRET) in Cy3/Cy5 mRNA. Huh-7 cells (50 000 cells/dish) were seeded on 35 mm glass-based dishes (Iwaki, Tokyo, Japan). Subcellular localization of polyplexes was investigated by incubating cells with Cellight Lysosome-GFP reagents for 16 h in 1 mL of DMEM containing 10% FBS. After replacement of media with fresh DMEM containing 10% FBS (1 mL), 90 μL of PAsp(DET) polyplex solution containing 3 μg of Cy3/Cy5 double-labeled mRNA (N/P = 10) was added. At 48 h after transfection, cells were washed with PBS and spectral imaging was performed using a super-resolution CLSM system (LSM 780: Carl Zeiss Co., Ltd., Oberlochen, Germany). The excitation wavelength for Cy3 and Cy5 was 561 nm, and that for GFP was 488 nm. Images were spectroscopically processed using the ZEN software (Carl Zeiss Co., Ltd., Oberlochen, Germany), and subcellular locations of polyplexes were determined according to GFP fluorescence.

Evaluation of Nuclease Resistance of mRNA in the Polyplexes Using FRET Analyses. Polyplex solutions containing Cy3/Cy5 double-labeled mRNA were incubated in MES (pH 5.5), HEPES (pH 7.2), or Tris-HCL (pH 9.0) buffer containing RNase A (50 μg/mL) for 1 h at 37 °C. Emission spectra for each polyplex were obtained using a NanoDrop ND-3300 fluorospectrometer (NanoDrop Technology) with excitation at 470 nm using a blue LED.

The FRET efficiency of each polyplex was calculated as follows:

$$\text{FRET efficiency} = \text{Cy3 (571nm) intensity}/\text{Cy5 (679nm) intensity}$$

FRET efficiency data were normalized to the differences between measurements taken at 0 and 1 h after addition of RNase A and are presented as the mean ± standard error of the mean from four samples.

Evaluation of Nuclease Resistance of mRNA Polyplexes Using Real Time Polymerase Chain Reaction (PCR). As in the previous section, polyplexes prepared from GLuc mRNA were incubated in MES (pH 5.5), HEPES (pH 7.2), or Tris-HCL (pH 9.0) buffer containing RNase A (5 μg/mL) for 1 h at 37 °C. Polyplex mRNA was collected using the RNeasy Mini Preparation Kit (Qiagen, Hilden, Germany) according to the manufacturer's protocol and reverse transcribed using the Quantitect Reverse Transcription Kit (Qiagen, Hilden, Germany). Subsequently, cDNA was quantified using real-time PCR with an ABI Prism 7500 instrument. The following primers were used to detect GLuc-specific sequences: forward, GGAGGTGCTCAAAGAGATGG and reverse, TTGAACCCAGGA-ATCTCAGG. Quantities of intact mRNA were expressed relative to that prior to incubation with RNase A.

Evaluation of Ethidium Bromide (EtBr) Intercalation into Polyplex mRNA. Polyplex solutions were mixed with EtBr (2.5 μg/mL) in MES (pH 5.5), HEPES (pH 7.2), or Tris-HCL (pH 9.0) buffer. After 1 h incubation at 37 °C, the fluorescence intensity at 590 nm was determined using a NanoDrop ND-1000 UV-meter (NanoDrop Technology) with excitation at 510 nm. Relative fluorescence was calculated as follows:

dx.doi.org/10.1021/ja506194z | J. Am. Chem. Soc. 2014, 136, 12396−12405

$$F = (F_{sample} - F_0)/(F_{100} - F_0)$$

where F_{sample}, F_{100}, and F_0 indicate the fluorescence intensity of the samples, free mRNA, and background, respectively.

Statistics. Significant differences between groups were identified using Student's t test and were considered significant when $p < 0.05$.

RESULTS AND DISCUSSION

Preparation and Characterization of N-Substituted Polyaspartamides. A series of N-substituted polyaspartamides bearing different number of side chain aminoethylene repeats (polycations) were synthesized by aminolysis reactions of β-benzyl groups of poly(β-benzyl-L-aspartate) (PBLA) with ethylenediamine (EDA), diethylenetriamine (DET), triethylenetetramine (TET), and tetraethylenepentamine (TEP) to produce poly[*N*-(2-aminoethyl)aspartamide] [PAsp(EDA)], poly{*N*′-[*N*-(2-aminoethyl)-2-aminoethyl]aspartamide} [PAsp(DET)], poly(*N*″-{*N*′-[*N*-(2-aminoethyl)-2-aminoethyl]-2-aminoethyl}aspartamide) [PAsp(TET)], and poly[*N*‴-(*N*″-{*N*′-[*N*-(2-aminoethyl)-2-aminoethyl]-2-aminoethyl}-2-aminoethyl)aspartamide] [PAsp(TEP)], respectively (Scheme 1).[9,10] This scheme of side chain aminolysis led to a synthesis of a series of polycations with same polymerization degrees and molecular weight distributions.

Changes in protonation of polycations between pHs corresponding to extracellular and endosomal pH (7.4 and 5.5, respectively) play a key role in endosomal escape of polyplexes because it determines the buffering capacity and cationic charge density of polycations, which affect interactions with cell membranes. Protonation of amino groups in the side chains of polycations can be estimated using potentiometric titrations from pH 1.2 to 11.5 (150 mM NaCl, 37 °C), as shown previously.[9]

Degrees of protonation (α) at pH 7.4 and 5.5, change in α from pH 7.4 to 5.5 ($\Delta\alpha$), and pK_a values for each polycation are summarized in Table 1. Protonated structures of side chains of each polycation were assumed from titrations, as illustrated in Scheme 2. Because PAsp(EDA) has a pK_{a1} of 9.0, its side chain is almost fully protonated at both pH values. In contrast, the major side chain in PAsp(DET) is monoprotonated at pH 7.4 and is diprotonated at pH 5.5, which crosses the pK_{a2} value of 6.2 between pH 7.4 and 5.5. The considerably low pK_{a2} value of PAsp(DET) is due to a strong electrostatic repulsion between two protonated amino groups in the diaminoethane unit, which hinders rotation according to the butane effect.[9] Likewise, the pK_{a3} value of PAsp(TET) is low due to intramolecular electrostatic repulsions, and eventually PAsp(TET) retains diprotonated side chains even at pH 5.5. The α (0.66) of PAsp(TET) at pH 5.5 is consistent with diprotonation of all side chains bearing $-CH_2CH_2-NH-CH_2CH_2-$ spacing. Because PAsp(TEP) has a pK_{a3} of 6.3 between pH 7.4 and 5.5, its major side chains are diprotonated at pH 7.4 and are triprotonated at pH 5.5. These pH-related changes in protonation of polycations reflect $\Delta\alpha$ values (Table 1), indicating that polycations bearing an even number of aminoethylene repeats (PA-Es), such as PAsp(DET) and PAsp(TEP), have larger $\Delta\alpha$ values and higher buffering capacity than those bearing an odd number of aminoethylene repeats (PA-Os), such as PAsp(EDA) and PAsp(TET).

Table 1. Degrees of Protonation (α) at pH 7.4 and 5.5, Changes in α from pH 7.4 to 5.5 ($\Delta\alpha$), and pK_a Values of N-Substituted Polyaspartamides

	α					
polycation	pH 7.4	pH 5.5	$\Delta\alpha$	pK_{a1}	pK_{a2}	pK_{a3}
PAsp(EDA)	0.93	0.99	0.06	9.0		
PAsp(DET)	0.51	0.82	0.31	8.9	6.2	
PAsp(TET)	0.56	0.66	0.10	9.1	7.8	4.3
PAsp(TEP)	0.49	0.68	0.19	9.0	8.2	6.3

Preparation of mRNA-Loaded Polyplexes from N-Substituted Polyaspartamides and Evaluation of Their Transfection Efficacy. Polyplexes loaded with Gaussia luciferase (GLuc) mRNA were prepared from polycations at the residual molar ratio of the polycation amino groups to mRNA phosphate groups (N/P) = 10. Hydrodynamic diameter and ζ-potential of these polyplexes are summarized in Supporting Information Table 1. All polyplexes showed similar size and ζ-potential of approximately 90 nm and 45 mV, respectively, regardless of the structure of polycations, indicating that the polyplexes possess similar physicochemical characteristics. Those polyplexes were then introduced into cultured human hepatoma cells (Huh-7). Transfection efficacy was evaluated over time by measuring the luminescence of secreted GLuc in the cell culture medium. Because GLuc has a half-life of 6 days in the medium,[13] luminescence assays accurately reflect cumulative GLuc expression over the incubation period. Until 12 h after mRNA introduction, PA-Es provided higher GLuc expression than PA-Os (Figure 1a). This is in a good accordance with our previous results obtained for pDNA transfection and can be explained by higher endosomal escape rates of PA-Es, which was due to the high buffering capacity and disruption of endosomal membranes induced by facilitated protonation, and particularly the formation of protonated side chain aminoethylene repeats with pH-drop in endosome.[9]

Unprecedentedly, 24 h after introduction of mRNA, a marked increase in GLuc expression was observed with the PA-Os polyplex PAsp(TET) (m = 3; Figure 1b), which produced the highest expression at 72 h among the four examined polyplexes. Similar increases in GLuc expression were observed after 10−12 h with the PA-O polyplex PAsp(EDA), which has fewer aminoethylene repeats (m = 1). However, the increase for PAsp(EDA) was less than that for PAsp(TET). Note that we also applied these mRNA polyplexes to mouse fibroblast-like cells (NIH3T3), and observed consistent expression profiles to Huh7, where PAsp(TET) provided a remarkable increase in expression 24 h after transfection (Supporting Information Figure 1). PAsp(TET) also had significantly lowered toxicity and higher transfection efficacy than a linear PEI-based commercial transfection reagent (ExGen 500; Figure 1b and Supporting Information Figure 2a). This observation indicates the practical significance of PAsp(TET) as a safe and efficient mRNA transfection reagent.

The increase in GLuc accumulation observed for PA-Os was inconsistent with our previous report, which showed greater endosomal escaping capability of PA-Es than PA-Os,[9] warranting further exploration of associated mechanisms. Cell viability after transfection and mRNA uptake did not differ significantly between the four polyplexes (Supporting Information Figure 2), excluding these factors from the reason for this trend. Then, we examined the translocation of mRNA from endosome to cytoplasm after transfection to estimate endosomal escaping capability of each polyplex. The intracellular distribution of Cy3-labeled mRNA loaded into the polyplexes

dx.doi.org/10.1021/ja506194z | J. Am. Chem. Soc. 2014, 136, 12396−12405

Scheme 2. Estimated Protonation of Side Chain Amino Groups in N-Substituted Polyaspartamides

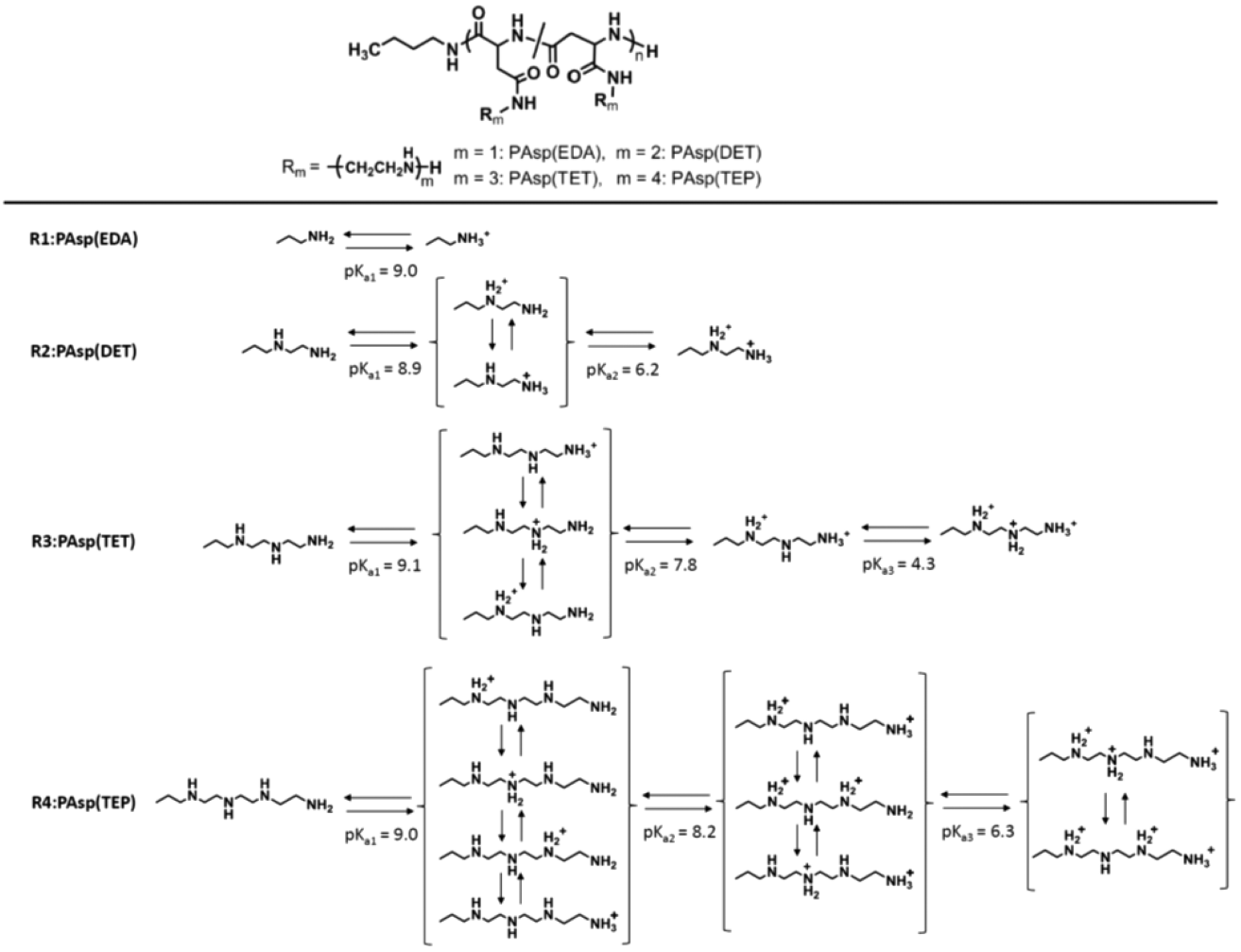

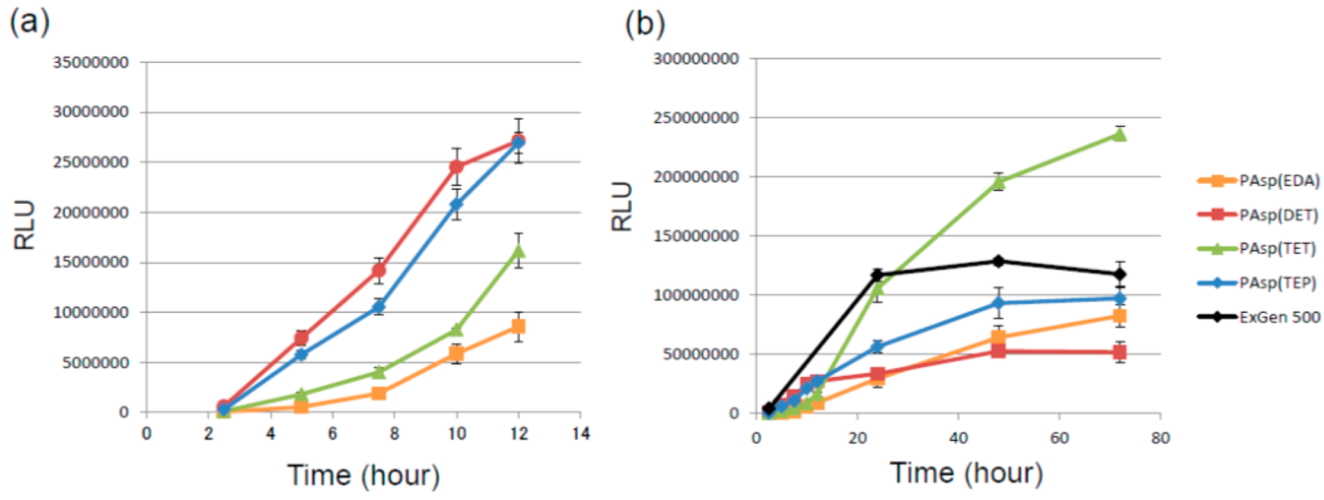

Figure 1. Cellular transfection of Gaussia luciferase (GLuc)-expressing mRNA using polyplexes prepared from N-substituted polyaspartamides. GLuc expression after transfection of mRNA polyplexes of PAsp(EDA), PAsp(DET), PAsp(TET), PAsp(TEP), or Exgen 500 into Huh-7 cells: (a) from 2 to 12 h and (b) from 2 to 72 h.

was analyzed by costaining of late endosomes and lysosomes using LysoTracker Green with a confocal laser scanning microscope (CLSM). Figure 2a–c shows typical CLSM images and indicates colocalization (yellow pixels) of Cy3-mRNA (red) with late endosomes and lysosomes (green). Colocalization ratios of the PA-Es PAsp(DET) and PAsp(TEP) were lower than those of the PA-Os PAsp(EDA) and PAsp(TET) at 12 h after transfection (Figure 2d), indicating higher capability of endosomal escape of PA-Es. This is consistent with higher Gluc expression from PA-Es than from PA-Os at 12 h (Figure

dx.doi.org/10.1021/ja506194z | J. Am. Chem. Soc. 2014, 136, 12396–12405

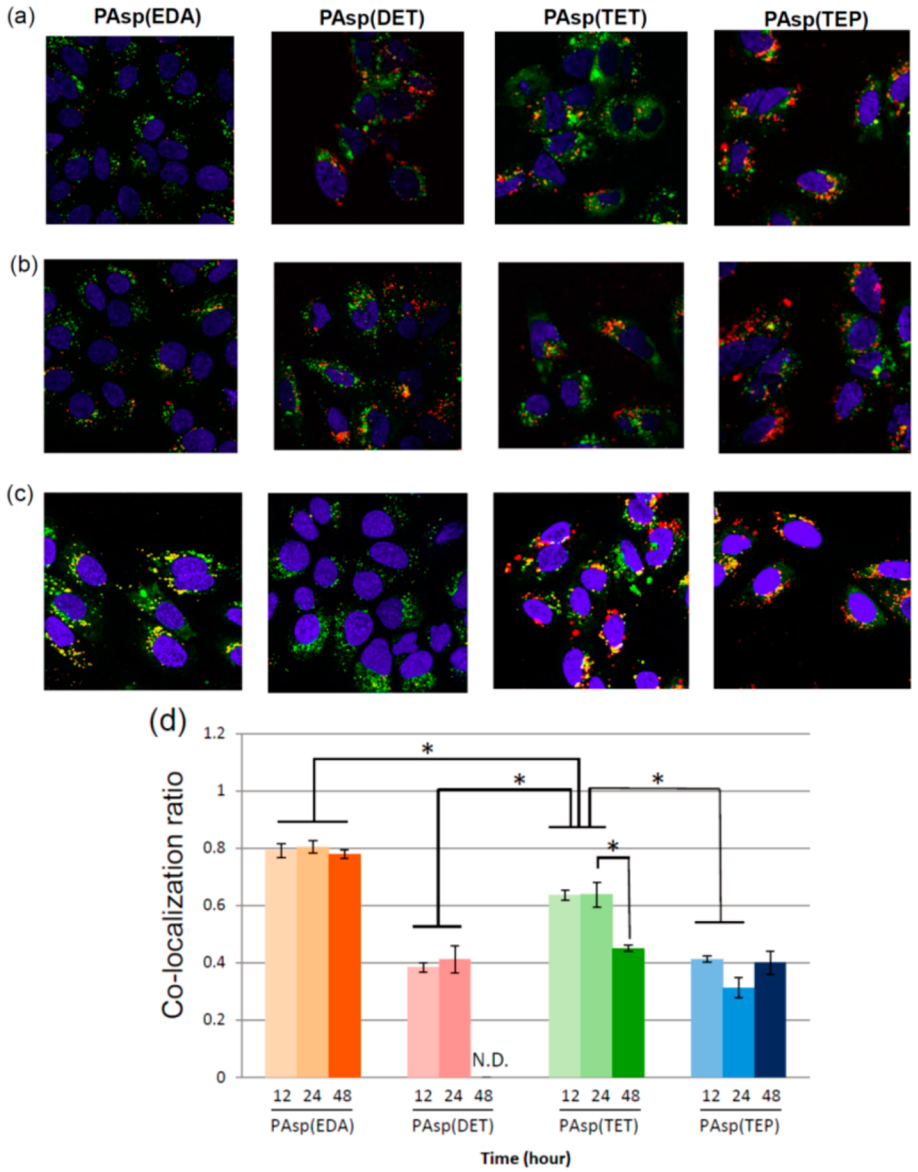

Figure 2. Colocalizatin of mRNA polyplexes with endosomes and lysosomes. Intracellular distribution of Cy3-labeled mRNA (red) polyplexes in Huh-7 cells at (a) 12, (b) 24, and (c) 48 h after transfection. Endosomes and lysosomes were stained with LysoTracker Green (green). Nuclei were stained with Hoechst 33342 (blue). (d) Colocalization ratios of Cy3-labeled mRNA with endosomes and lysosomes were calculated from fluorescent cell images taken using LSM software at 12, 24, and 48 h after transfection.

1a) and reflects acidic pH-sensitive endosomal membrane destabilization.[8,9] A significant decrease in the colocalization ratio of mRNA in late endosomes and lysosomes (green) was observed at 48 h after PAsp(TET) transfection, and this corresponded with increased GLuc expression (Figure 1b). It may be reasonable to assume that the delayed translocation of mRNA from endosomes to the cytoplasm caused the prolonged induction period of GLuc expression of PAsp(TET). As previously reported, escaping ability from acidic endosomes of polyplexes prepared form N-substituted polyaspartamides with side chain aminoethylene repeats is related to their membrane disruption activity, as evaluated from the hemolysis assays.[9] PA-Es induced significant hemolysis at pH 5.5, whereas PA-Os did not cause hemolysis under these conditions (Supporting Information Figure 3). This trend is consistent with the larger pH dependent increments of protonation ($\Delta\alpha$, pH 7.4−5.5) of the PA-Es PAsp(DET) and PAsp(TEP) compared with those of the PA-Os PAsp(EDA) and PAsp(TET), as indicated in potentiometric titrations (Table 1). However, even PAsp(TET) appeared to have hemolysis activity with further decrease in the surrounding pH from 5.5 to 5.0. Because the $\Delta\alpha$ of PAsp(TET) substantially increases between pH 5.0 and 5.5, facilitated protonation of aminoethylene repeats in the PAsp(TET) side chain may be responsible for the delayed translocation of PAsp(TET) into the cytoplasm (Supporting Information Table 2). As the drop in intravesicular pH is known to take time along the endocytic pathway from pH 6.0−6.5 in early endosomes to pH 4.5−5.5 in late endosomes and lysosomes,[14] delayed PAsp(TET)-mediated GLuc expression compared with that of PA-Es likely reflects the time course of polyplex translocation from vesicular compartments in response to decreased intravesicular pH.

PAsp(EDA), which also belongs to PA-Os, revealed similar tendencies to the PAsp(TET) system with delayed onset of GLuc expression. However, transfection efficacy was significantly lower than that for PAsp(TET), presumably because of

dx.doi.org/10.1021/ja506194z | J. Am. Chem. Soc. 2014, 136, 12396−12405

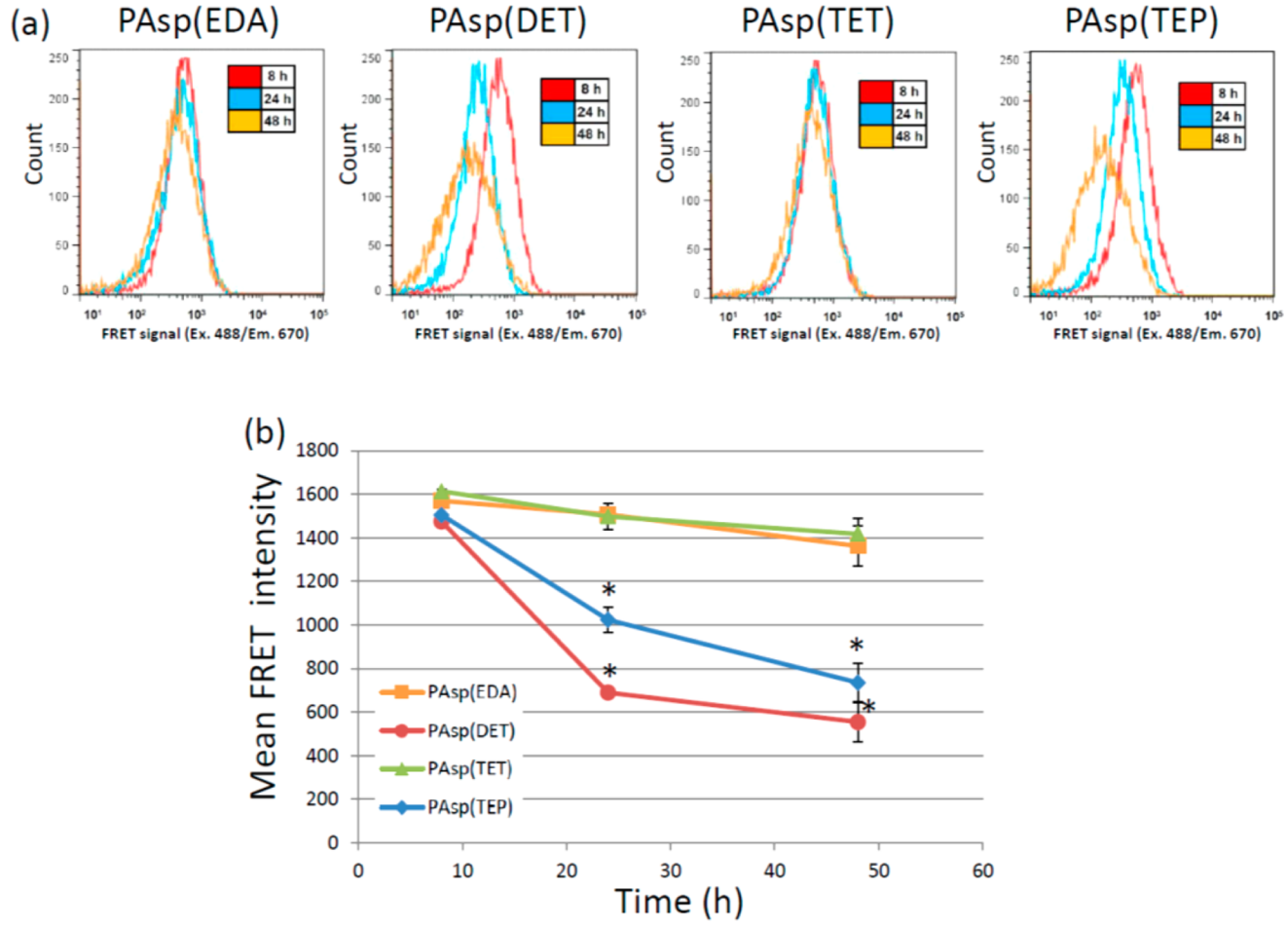

Figure 3. Intracellular fluorescence resonance energy transfer (FRET) analysis of Cy3/Cy5 double-labeled mRNA by flow cytometry after mRNA transfection. (a) Histograms of FRET signals analyzed by flow cytometry at 8, 24, and 48 h after Cy3/Cy5 double-labeled mRNA transfection of Huh-7 cells with PAsp(EDA), PAsp(DET), PAsp(TET), or PAsp(TEP) polyplex. The samples were excited with a 488 nm laser, and their emission was monitored by using a 660/20 filter. (b) Mean FRET intensity values in Huh-7 cells transfected by each polyplex were calculated at 8, 24, and 48 h from three individual experiments. Asterisk (*) indicates PA-Es showing significantly lower FRET intensity than PA-Os ($P < 0.05$).

limited endosomal escape even after 48 h (Figure 2d). This observation was consistent with our previous experiments with pDNA polyplexes, indicating that at least two protonated amino groups are required in the side chain to exert effective membrane interactions.[9]

The delayed onset in mRNA expression observed for PA-Os compared to PA-Es may be adequately explained by their slow endosomal escaping behaviors as supported by CLSM observation. However, these data do not indicate greater facilitated expression with PA-Os compared with that with PA-Es after 24 h transfection because PA-Es should have more fractions in the cytoplasm even from the early stage of transfection attributed to their superior endosomal escaping function. In this regard, it is worth noting that no mRNA was detectable in microscopy images of cytoplasmic PAsp(DET) after 48 h (Figure 2c), precluding calculation of colocalization ratios (Figure 2d). This phenomenon may reflect rapid degradation of mRNA in the cytoplasm because of instability of the polyplex. In line with this view, GLuc concentrations plateaued 24 h after transfection with the PAsp(DET) system (Figure 1b). Given the relatively long half-life of GLuc in the medium (approximately 6 days),[13] this observation indicates cessation of GLuc expression in the later time period for the PAsp(DET) system. On the other hand, continuous increases in GLuc concentrations were observed for the other three systems, indicating appreciable viability of mRNA in the cytoplasm. To get more insight in the mechanisms involved in this mRNA expression profile, we directly examined the stability of mRNA polyplexes inside cells using fluorescence resonance energy transfer (FRET).

Stability of mRNA Polyplexes in Cells: FRET Analyses of Cy3/Cy5 Double-Labeled mRNA. Because FRET efficiency should correlate with the condensation level of double-labeled mRNA, it can reflect the status of mRNA of the polyplexes in cells.[15−17] Therefore, we analyzed FRET of Cy3/Cy5 double-labeled mRNA by flow cytometry. After 8, 24, and 48 h of double-labeled mRNA transfection, FRET intensity of cells was measured by exciting the cells with a 488 nm laser and monitoring the fluorescence emission through a 660/20 nm filter. Histogram plots of FRET signal of each polycation are illustrated in Figure 3a. The histogram of PA-Es shifted more rapidly than that of PA-Os. Moreover, the mean FRET intensity of each polyplex was calculated by using FACSDiva software from individual three experiments at each time point (Figure 3b). As shown in Figure 3b, a clear odd−even effect on mean FRET intensity was observed, whereas all polyplexes showed similar cellular uptake at 24 h (Supporting Information Figure 2b). Although PA-Os maintained high FRET intensity

dx.doi.org/10.1021/ja506194z | J. Am. Chem. Soc. 2014, 136, 12396−12405

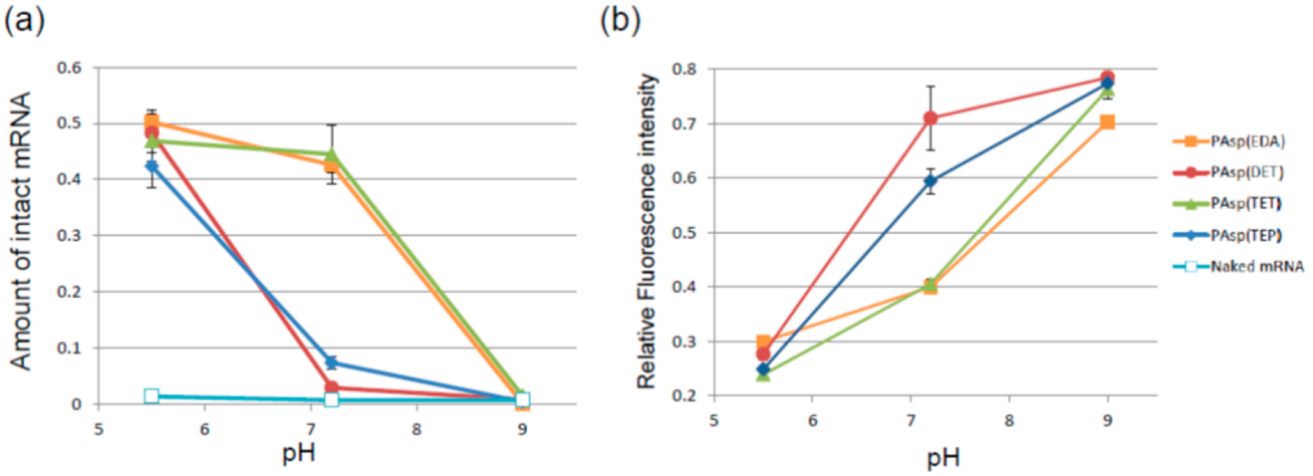

Figure 4. Evaluation of mRNA properties in the polyplexes. (a) Stability of mRNA against nuclease attack after incubation with RNase at pH 5.5, 7.2, or 9.0. (b) Ethidium bromide (EtBr) accessibility to polyplex mRNA at pH 5.5, 7.2, or 9.0.

until 48 h, FRET intensity of PA-Es decreased significantly within 24 h. This quantitative FRET analyses clearly revealed that PA-Es have lower stability in the cells and rapidly released mRNA to allow facilitated GLuc expression at the initial stage of transfection. Because the half-life of endogenous cytoplasmic mRNA in mammalian cells is estimated to several hours (median; 9 h),[18] the most plausible reason to explain the rapid decrease of PAsp(DET) FRET intensity may relate to rapid degradation of mRNA. This view is supported by the termination in GLuc production in PAsp(DET)-transfected cells after 24 h, as indicated by plateauing of GLuc accumulations (Figure 1b). In contrast, the slow and sustained escape of PA-Os from endo/lysosomal compartments and their high stability in the cells (high FRET intensities) are consistent with the observations of continuous GLuc expression. In this context, the further question was arisen from CLSM observation. At 48 h, PAsp(DET) polyplexes disappeared from cytoplasm but still remained in lysosome. To clarify this mechanism, we used a super-resolution CLSM system (LSM780, Carl Zeiss Microscopy Co., Ltd., Oberlochen, Germany) that enables analyses of Cy3 (green) and Cy5 (red) double-labeled mRNA in lysosomes costained with CellLight Lysosomes-GFP (blue; Supporting Information Figure 4). In the CLSM image, PAsp(DET) polyplexes showed the yellow pixels which reflect the colocalization of Cy3 (green) and Cy5 (red) pixels, in lysosome after 48 h transfection. This observation suggested that the mRNA in lysosome may be stably packed in PAsp(DET) polyplexes.

Enhanced Nuclease Resistance of Polyplex mRNA. To elucidate mechanisms relating to odd−even differences in stability of the polyplexes, we investigated the resistance of mRNA in the polyplexes against RNase in buffer at pH 9.0, 7.2 (cytoplasmic environment), and 5.5 (endosomal/lysosomal environment), because endonucleolytic cleavage is an important process of cytoplasmic mRNA decay.[19,20] At pH 5.5, mRNA remained intact in all the polyplexes after 1 h incubation with RNase-containing buffer (Figure 4a). In contrast, free mRNA was completely degraded, indicating substantial stability of all polyplexes under acidic conditions. This is consistent with FRET observation using CLSM (Supporting Information Figure 4) indicating a highly condensed state of mRNA in polyplexes in endosome and lysosome environments. In contrast, under nonphysiological alkaline condition (pH 9.0), mRNA in all polyplexes was completely degraded. Apparently, the protonated fraction of amino groups in the side chain dramatically decreases in alkaline condition, thereby resulting in loosening or possibly partial dissolution of the polyplex structure to allow enzyme attack toward mRNA. Indeed, the accessibility of intercalating dye, ethidium bromide (EtBr), to mRNA in the polyplexes significantly increased by changing pH from 5.5 to 9.0 as judged from an increase in relative fluorescence intensity of EtBr within mRNA (Figure 4b). Worth noting in this assay of mRNA stability against RNase is a clear difference at physiological condition (pH = 7.2) between PA-Os and PA-Es: mRNA in the PA-Es PAsp(DET) and PAsp(TEP) was almost completely degraded similarly to free mRNA, whereas that in the PA-Os PAsp(EDA) and PAsp(TET) remained intact as is the case with the result obtained at pH 5.5. EtBr assays (Figure 4b) indicated that mRNA forms more condensed structures in PA-Os than in PA-Es. Moreover, FRET analysis using the doubly labeled mRNA with Cy3 and Cy5 in RNase-containing buffer also demonstrated higher FRET efficienty for PA-Os than for PA-Es at pH 7.2 (Supporting Information Figure 5), confirming greater stability of PA-Os against RNase attack.

Proposed Mechanism of mRNA Stabilization in PA-O Polyplexes. All the present polyplexes protected mRNA from RNase attack in acidic endosomal compartments (Figure 4a and Supporting Information Figure 4). Then, smooth translocation into the cytoplasm occurs for PA-Es, even from early endosomes with a pH of approximately 6.0, reflecting facilitated protonation of diaminoethane repeats to form the diprotonated diaminoethane unit ($-NH_2^+-CH_2-CH_2-NH_2^+-$) (Scheme 2). In titration experiments, ratios of PAsp(DET) and PAsp(TEP) side chains comprising fully protonated diaminoethane units ($-NH_2^+-CH_2-CH_2-NH_2^+-$) were 40% and 52%, respectively, even at pH 6.0. Alternatively, translocation into cytoplasm is slow and limited for PA-Os as judged from the colocalization data in Figure 2d. Significant drop in the colocalization ratio for the PAsp(TET) at the later time period (48 h) is consistent with the hypothesis that appreciable pH drop in the late ensosome/lysosome (pH ∼ 4.5) may facilitate the escape of polyplexes into the cytoplasm with the formation of the fully protonated array of the amino groups ($-NH_2^+-CH_2-CH_2-NH_2^+-CH_2-CH_2-NH_3^+$) in the side chain. Note that the fraction of PAsp(TET) side chain with a fully

dx.doi.org/10.1021/ja506194z | J. Am. Chem. Soc. 2014, 136, 12396−12405

protonated structure is calculated to be 21% at pH 4.5 from the value of pK_{a3}= 4.3. Escape of PAsp(EDA) into the cytoplasm may be limited because the absence of the repetitive protonated array is expected for the structure of this polyplex.

Although all the polyplexes offered significant protection against RNase attack under acidic conditions (pH 5.5; Figure 4a), a clear odd−even effect was observed in mRNA protection at pH 7.2, with PA-Os offering far greater stability than PA-Es. Moreover, this odd−even effect on RNase stability of loaded mRNA in the polyplexes reasonably explains their distinct behavior observed in cell experiments, and certainly worth discussing the mechanisms involved in this interesting phenomenon. As can be seen in Scheme 2, side chains of each polycation take variable protonated structures depending on pH. It is thus reasonable to assume that this variation in the protonation may play a role in the stability of mRNA in polyplexes.

Here, we focus on the pH-sensitive change in the protonation of the terminal primary amino groups. They are essentially fully protonated at pH 5.5 for all the polycations (Scheme 2), and only a fraction of primary amino groups in the PA-Es PAsp(DET) and PAsp(TEP) should be nonprotonated at pH 7.2. Given the α values of PAsp(DET) and PAsp(TEP) (0.51 and 0.49, respectively) and the feasibility of side chain protonation, half and one-third of the primary amino groups may be in the nonprotonated form on PAsp(DET) and PAsp(TEP), respectively. In contrast, primary amino groups of the PA-Os PAsp(EDA) and PAsp(TET) are almost fully protonated under these conditions. These differences in protonation of terminal primary side chain amino groups correlate with the nuclease resistance of polyplexes as follows: PAsp(EDA) = PAsp(TET) > PAsp(TEP) > PAsp(DET). Although further molecular assessments are required to elucidate details of this mechanism, the cationic charge at the end of the side chain appears indispensable to the stability of polyplex structures, particularly under nuclease attack.

CONCLUSION

The present data show that endosomal escape rates and cytoplasmic stability are important trade-off parameters determining the ultimate transfection efficacy of mRNA-loaded polyplexes formed from N-substituted polyaspartamides. Sustained protein expression was achieved by polyplexes with an odd number of aminoethylene repeats (PA-Os). This reflected stability in the cytoplasm and compensated for their inferior endosome escape rates. In contrast, polyaspartamides with an even number of aminoethylene repeats (PA-Es) showed abrupt changes in protonation between external and endosomal pH conditions, producing high enodosome escape rates. However, their poor stability in cytoplasmic condition impairs their function to sustainably express coded proteins. We previously examined pDNA-loaded polyplexes from the same series of *N*-polyaspartamide derivatives evaluated in this study[9] and showed that PA-Es had greater transfection efficiency than PA-Os. Therefore, the key transfection process to determine the efficacy may differ between mRNA and pDNA delivery systems, potentially reflecting differences in the inherent stability of mRNA and pDNA polyplexes. Higher cytoplasmic stability of pDNA compared to mRNA may shift the limiting step in transfection from the cytoplasmic stability to the efficacy of endosomal escape, thereby giving an opposite odd−even effect in transfection efficacy. These findings show that the chemistry-based design with fine-tuning in the structure of polycation to construct polyplexes is indispensably important to develop mRNA and pDNA delivery systems that may have future clinical applications.

ASSOCIATED CONTENT

Supporting Information

Additional tables with hydrodynamic diameter (D_H), polydispersity index (PDI), and ζ-potential of polyplexes, and protonation degree and $\Delta\alpha$ of N-substituted polyaspartamides. Figures showing data for GLuc expression after transfection of messenger RNA, cell viability and cellular uptake assays, hemolysis assay, FRET evaluation of Cy3/Cy5 double-labeled mRNA, and FRET efficiency of each polyplex after incubation in buffers containing RNase. This material is available free of charge via the Internet at: http://pubs.acs.org.

AUTHOR INFORMATION

Corresponding Author

kataoka@bmw.t.u-tokyo.ac.jp

Notes

The authors declare no competing financial interest.

ACKNOWLEDGMENTS

This work was financially supported in part by the Center of Innovation Program from Japan Science and Technology Agency (JST), the Funding Program for World-Leading Innovation R&D on Science and Technology (FIRST) from Japan Society for the Promotion of Sciences (JSPS), JSPS KAKENHI Grant-in-Aid for Specially Promoted Research (Grant Number 25000006 (K.K.)), Grant-in-Aid for Scientific Research (B) (Grant Number 24300170 (K.I.)), Grant-in-Aid for Research Activity Start-up (Grant Number 24800016 (H.U.)), and JSPS Core-to-Core Program, A. Advanced Research Networks. We thank Katsue Morii, Asuka Miyoshi, and Sae Suzuki (The University of Tokyo) for their technical assistance.

REFERENCES

(1) Kormann, M. S.; Hasenpusch, G.; Aneja, M. K.; Nica, G.; Flemmer, A. W.; Herber-Jonat, S.; Huppmann, M.; Mays, L. E.; Illenyi, M.; Schams, A. *Nat. Biotechnol.* **2011**, *29*, 154.

(2) Tavernier, G.; Andries, O.; Demeester, J.; Sanders, N. N.; De Smedt, S. C.; Rejman, J. *J. Controlled Release* **2011**, *150*, 238.

(3) Kabanov, A.; Kabanov, V. *Bioconjugate Chem.* **1995**, *6*, 7.

(4) Kakizawa, Y.; Kataoka, K. *Adv. Drug Delivery Rev.* **2002**, *54*, 203.

(5) Pack, D. W.; Hoffman, A. S.; Pun, S.; Stayton, P. S. *Nat. Rev. Drug Discovery* **2005**, *4*, 581.

(6) Mastrobattista, E.; van der Aa, M. A.; Hennink, W. E.; Crommelin, D. J. *Nat. Rev. Drug Discovery* **2006**, *5*, 115.

(7) Green, J. J.; Langer, R.; Anderson, D. G. *Acc. Chem. Res.* **2008**, *41*, 749.

(8) Miyata, K.; Oba, M.; Nakanishi, M.; Fukushima, S.; Yamasaki, Y.; Koyama, H.; Nishiyama, N.; Kataoka, K. *J. Am. Chem. Soc.* **2008**, *130*, 16287.

(9) Uchida, H.; Miyata, K.; Oba, M.; Ishii, T.; Suma, T.; Itaka, K.; Nishiyama, N.; Kataoka, K. *J. Am. Chem. Soc.* **2011**, *133*, 15524.

(10) Suma, T.; Miyata, K.; Ishii, T.; Uchida, S.; Uchida, H.; Itaka, K.; Nishiyama, N.; Kataoka, K. *Biomaterials* **2012**, *33*, 2770.

(11) Miyata, K.; Nishiyama, N.; Kataoka, K. *Chem. Soc. Rev.* **2012**, *41*, 2562.

(12) Wattiaux, R.; Laurent, N.; Wattiaux-De Coninck, S.; Jadot, M. *Adv. Drug Delivery Rev.* **2000**, *41*, 201.

(13) Wurdinger, T.; Badr, C.; Pike, L.; de Kleine, R.; Weissleder, R.; Breakefield, X. O.; Tannous, B. A. *Nat. Methods* **2008**, *5*, 171.

(14) Sorkin, A.; von Zastrow, M. *Nat. Rev. Mol. Cell Biol.* **2002**, *3*, 600.
(15) Itaka, K.; Harada, A.; Nakamura, K.; Kawaguchi, H.; Kataoka, K. *Biomacromolecules* **2002**, *3*, 841.
(16) Itaka, K.; Harada, A.; Yamasaki, Y.; Nakamura, K.; Kawaguchi, H.; Kataoka, K. *J. Gene Med.* **2004**, *6*, 76.
(17) Matsumoto, Y.; Itaka, K.; Yamasoba, T.; Kataoka, K. *J. Gene Med.* **2009**, *11*, 615.
(18) Schwanhäusser, B.; Busse, D.; Li, N.; Dittmar, G.; Schuchhardt, J.; Wolf, J.; Chen, W.; Selbach, M. *Nature* **2011**, *473*, 337.
(19) Schoenberg, D. R. *Wiley Interdiscip. Rev.: RNA* **2011**, *2*, 582.
(20) Schoenberg, D. R.; Maquat, L. E. *Nat. Rev. Genet.* **2012**, *13*, 246.